Published in final edited form as:
Biofouling. 2011 May ; 27(5): 505–518. doi:10.1080/08927014.2011.585711.

Competitive Protein Adsorption on Polysaccharide and Hyaluronate Modified Surfaces

Michela Ombelli[a], **Lauren Costello**[b], **Corinne Postle**[a], **Vinod Anantharaman**[a], **Qing Cheng Meng**[a], **Russell J. Composto**[b], and **David M. Eckmann**[a,*]

[a]Department of Anesthesiology and Critical Care, University of Pennsylvania, Philadelphia, PA 19104

[b]Department of Material Science and Engineering, University of Pennsylvania, Philadelphia, PA 19104

Abstract

We measured adsorption of bovine serum albumin (BSA) and fibrinogen (Fg) onto six distinct bare and dextran- and hyaluronate-modified silicon surfaces created using two dextran grafting densities and three hyaluronic acid (HA) sodium salts derived from human umbilical cord, rooster comb and streptococcus zooepidemicus. Film thickness and surface morphology depended on HA molecular weight and concentration. BSA coverage was enhanced on surfaces upon competitive adsorption of BSA:Fg mixtures. Dextranization differentially reduced protein adsorption onto surfaces based on oxidation state. Hyaluronization was demonstrated to provide the greatest resistance to protein coverage, equivalent to that of the most resistant dextranized surface. Resistance to protein adsorption was independent of the type of hyaluronic acid utilized. With changing bulk protein concentration from 20 to 40 μg ml^{-1} for each species, Fg coverage on silicon increased by 4×, whereas both BSA and Fg adsorption on dextran and HA were far less dependent of protein bulk concentration.

Keywords

Competitive protein adsorption; HPLC; biocompatible surfaces; dextran; hyaluronate; biofouling

Introduction

A universal definition of biocompatibility for devices and indwelling biomaterials, particularly for those in direct contact with blood, has yet to be established (Castner and Ratner 2002). However, device or implant failure has been consistently linked to biomaterial and biomedical device surfaces that provoke blood clotting, tissue inflammation, and infection (Edmunds, Jr. et al. 2003). Blood contact with a biomaterial initiates rapid adsorption of plasma proteins, which often elicits the foreign body reaction heralded by a massive inflammatory response. Albumin and fibrinogen, two major blood proteins, are among those first molecules selectively adsorbed. Their concentrations and the concentrations of other adsorbed proteins on a surface continually vary. As the molecules compete for surface occupancy sites, they become tightly packed, and may become irreversibly bound and immobilized on the interface (Edmunds, Jr. et al. 2003). Adsorbed plasma proteins can also change conformation, relative to their bulk structure, to a limited

*To whom correspondence should be addressed at the Department of Anesthesiology and Critical Care, 331 John Morgan Building, University of Pennsylvania, Philadelphia, PA 19104. eckmanndm@uphs.upenn.edu.

degree such that “receptor” amino acid sequences are exposed. These sequences can provide signals that are specifically recognized by cells or by other macromolecules circulating in blood, leading to initiation of thrombogenesis, platelet adhesion, platelet aggregation, as well as complement activation leading to leukocyte aggregation (Castner and Ratner 2002; Edmunds, Jr. et al. 2003) or other biological responses.

Numerous experimental techniques have been developed both to identify the type of, and quantify the amount of, physisorbed proteins (Horbett and Brash 1995). Analytical approaches to study protein adsorption have included use of radioactive labels (Dejardin et al. 1995; Grunkemeier et al. 2000; Grunkemeier et al. 2001; Jenney and Anderson 2000; Martins et al. 2003; Tsai et al. 1999; Tsai et al. 2002; Tsai and Horbett 1999), fluorescence tagging (Kim and Somorjai 2003; Toworfe et al. 2004), gel electrophoresis and immunoblot analysis (Babensee et al. 1998; Cornelius et al. 2003; Cornelius and Brash 1999; Klomp et al. 1999; Weber et al. 2001), total internal reflection fluorescence and *in situ* ellipsometry (Lassen and Malmsten 1996a; Lassen and Malmsten 1996b; Lassen and Malmsten 1997), and electron spectroscopy for chemical analysis and time-of-flight secondary ion mass spectrometry to characterize surfaces containing multiple types of adsorbed proteins (Wagner et al. 2003a; Wagner et al. 2003b).

We have previously demonstrated that high-performance liquid chromatography (HPLC) is an effective tool for investigating protein adsorption from multicomponent mixtures onto biomaterial surfaces (Ombelli et al. 2005). HPLC chromatograms yield both quantitative and qualitative information via peak area and retention time, respectively, for analysis of protein mixtures. Since HPLC is an *ex situ* technique, the adsorbed proteins must be completely removed from the surface for accurate measurements to be made. In our approach, very nearly 100% of the adsorbed proteins studied are removed by rinsing the surfaces with CHAPS (3-[(3-cholamidopropyl)dimethylammonio]-1-propanesulfonate), which solubilizes membrane proteins while preserving their native structure (Engel et al. 2003).

We have also been pursuing new synthetic surface coatings that provide reproducible control of surface chemical composition and structural morphology. We seek to create biomaterial coatings that incorporate molecular elements of the vascular endothelial surface layer, or glycocalyx. This particular biological structure is composed of polysaccharides and proteoglycans (Cryer 1983)}, which have previously been studied as coatings for biomaterials (Dai et al. 2000; Hartley et al. 2002; Mason et al. 2000). The endothelial glycocalyx surface layer is particularly rich in hyaluronic acid (HA), making it an attractive molecule to study for vascular biomaterial applications. The glycocalyx in general merits this attention since it serves as the direct molecular interface mediating contact between circulating blood and the vessel wall. Providing a biomaterial surface structure that includes molecular constituents of the endothelial cell surface layer should help to confer the protection from adverse physiological responses that is afforded naturally by the glycocalyx *in vivo*.

In previous studies we demonstrated our ability to prepare dextran coatings in which we controlled thickness, wettability and roughness by varying molecular weight, polydispersity (Ombelli et al. 2002; Ombelli et al. 2003) and degree of oxidation (Miksa et al. 2004; Miksa et al. 2006). We now extend that work to evaluate competitive adsorption of bovine serum albumin (BSA) and bovine fibrinogen (Fg) onto dextranized as well as introduce competitive adsorption on sodium hyaluronate (HA) coatings. Consistent with prior studies (Ombelli et al. 2005), sparsely grafted dextran is more effective than tightly bound (high grafting density) dextran in suppressing individual and total protein adsorption. The hyaluronized surfaces are equally effective as the sparsely grafted dextran layers at reducing

protein adsorption. In competitive adsorption studies, dextranized and hyaluronized surfaces attract a greater mass of BSA than Fg to their surfaces.

Experimental

Materials and methods

All reagents and solvents were used as received unless otherwise stated. Aminopropyltriethoxysilane (APTES), sodium periodate, 99% ($NaIO_4$), sodium cyanoborohydrate ($NaBH_3CN$), and dimethylformamide were purchased from Sigma-Aldrich Co. Dextran prepared from Leuconostoc ssp (Mw = 110,000, Mw Mn^{-1} = 1.52) was supplied by Fluka Chemie. All Sodium Hyaluronate (NaHA) was obtained by Sigma: Hyaluronic Acid Sodium Salt from Human Umbilical Cord (ref H1876, lot 092K1070, molecular weight 3–5.8 million), Hyaluronic Acid Sodium Salt from Rooster Comb (ref H5388, molecular weight 1.3–2.0 million), and Hyaluronic Acid Sodium Salt from Streptococcus Zooepidemicus (ref H9390, molecular weight 0.85–1.6 million). N-Ethyl-N'-(3-dimethylaminopropyl) carbodiimide (EDC, Sigma, 39391), and N-Hydroxysuccinimide (NHS, Sigma, 13,067-2) were used in attaching the NaHA to the surface. The identical batch of streptococcus zooepidemicus NaHA was investigated previously by Tadmor et al. (Tadmor et al. 2002) and found to have a viscosity average molecular weight of 540k in 0.1M NaCl solution and an overlap concentration of 0.8 mg ml^{-1} in HEPES buffer, which was deemed a "very good solvent for the HA." Moreover a persistence length of 4.5 to 9 nm was noted. For good solvent conditions the overlap concentration for the other NaHA molecular weight is given by $c^*(M) = c^*(540k)\,(M(540k)^{-0.8}$. Correspondingly, the rooster comb and human NaHA's have overlap concentrations of 0.4 to 0.3 and 0.2 to 0.1 mg ml^{-1}, respectively. Note that the overlap concentration decreases as the chain size increases, indicating that the longer chains begin to entangle at lower concentrations than do the shorter ones.

Double side polished silicon wafers having a surface area of ~40 cm^2 for protein adsorption studies and single side polished silicon wafers measuring 35 mm × 15 mm for zeta potential measurement were purchased from Silicon Quest Int'l (Santa Clara, CA). BSA, lyophilized, fatty acids- and globulin-free was obtained from Sigma Chemical Co., USA, as were Fg (fraction I; >75% clottable protein) and CHAPS (Sigma C3023). The proteins, selected based on our previous development of the HPLC method for protein quantification (Ombelli et al. 2005), were used without further purification. For surface preparation, the water came from a Millipore® filtration system and had a resistivity of 18.2 mΩ. To prepare protein solutions and clean the experimental apparatus, water came from a Barnstead Mega-Pure® MP-1 water purification system.

Surface Preparation

Dextranized Surfaces

We prepared dextranized silicon wafers using the experimental method detailed in previous publications (Miksa et al. 2004; Miksa et al. 2006; Ombelli et al. 2002; Ombelli et al. 2003; Ombelli et al. 2005). The dextranized surface for this experiment was obtained by oxidizing dextran for either 0.5 or 4 h prior to grafting on amino-functionalized silicon, with full detail of the method having been previously reported (Miksa et al. 2006). These two oxidation times were selected because they were shown to yield surfaces having similar wettability, roughness and thickness but different adhesion force characteristics indicating the onset of multilayer dextran formation for the longer oxidation time (Miksa et al. 2006). Briefly, our dextran grafting procedure requires silicon surfaces first be etched clean by immersion in "piranha" solution (70% H_2SO_4 and 30% H_2O_2, v v^{-1}). After washing with, and soaking in, water, surfaces were dried with compressed N_2(g) and exposed to ultra violet light in a

UVO-Cleaner (Model 144A, Jelight Company Inc.; Irvine, CA). The resultant homogeneous silanol layer was reacted with APTES deposited by vapor deposition under inert atmosphere in a glove box. To control the grafting density of dextran on APTES, aqueous dextran solutions (1 mg ml^{-1}) were prepared and oxidized for the predetermined time (0.5 or 4 h) before being transferred to a beaker containing $NaBH_3CN$. After mixing, these solutions were transferred to Petri dishes containing APTES modified silicon wafers, which were left on an orbital shaker overnight. Subsequently, the wafers were removed from solution and were washed with, and sonicated in, water.

Hyaluronized Surfaces

We prepared hyaluronized silicon wafers using the chemistry depicted in Figure 1. Concentrations of NaHA in the range of 0.2 mg ml^{-1} to 3.4 mg ml^{-1} dissolved in 15 ml of Millipore H_2O. For reference, the upper concentration limit corresponds to the concentration of NaHA in synovial fluid. NHS, measured in the glovebox, was dissolved in 3 ml of Millipore H_2O. Once dissolved, the EDC and Millipore H_2O were added to the NHS+H_2O and raised to a volume of 5 ml. The ratio of NHS to EDC (40 mM:20 mM) was based on published literature values (Stile et al. 2002). The NaHA was dissolved in Millipore H_2O and 1 μl of hydrochloric acid (HCl; Fischer Scientific) was added to lower the pH of the solution from 6.1 ± 0.2 to 4.1 ± 0.6. Once the NaHA was completely dissolved, the EDC and NHS were added to bring the reaction volume to 20 ml. The etched silicon wafers, prior to incubation, were immersed in Phosphate Buffered Saline (PBS; Sigma, theoretical pH 7.4) on a shaker for ten minutes and rinsed with Millipore H_2O. The immobilization reaction proceeded at room temperature on a shaker for 20 hr. Following the incubation time, all surfaces were washed with Millipore H_2O and sonicated for 20 min in Millipore H_2O.

Surface Characterization

Results for dextranized surface characterization including ellipsometry, atomic force microscopy and contact angle measurement have previously been reported (Miksa et al. 2006). Surface characterization of hyaluronized surfaces by multiple modalities is described below, as is the XPS and zeta potential analysis of both the dextranized and hyaluronized surfaces.

Ellipsometry

The dried film thickness of NaHA at the three different molecular weights was measured as a function of NaHA concentration using a Rudolph Research AutoEL-II ellipsometer. These initial studies were conducted to guide selection of the optimum NaHA molecular weight and concentration for protein adsorption experiments. Measurements were performed on three separate samples, with mean values and standard deviations plotted in Figure 2. Solution concentrations for immersion ranged from dilute (below c*, the overlap concentration) to semi-dilute (up to a maximum of 3.4 mg ml^{-1}). For the two highest molecular weight NaHA subtypes, layer thickness increases strongly for concentrations greater than the overlap but decreased after a concentration of 1.2 mg ml^{-1} is reached. This initial increase may result from the dramatic increase in viscosity above the overlap concentration whereas the decrease might result from slower relaxations and reduced reactivity near the crowded surface. Further studies are needed to understand the mechanism underlying these observations. Other than the thickness at 1.2 mg ml^{-1}, the streptococcus zooepidemicus NaHA was relatively insensitive to solution concentration, averaging about 50 nm from 0.2 to 3.4 g ml^{-1}. Human NaHA produced the thickest films and streptococcus zooepidemicus NaHa produced the thinnest films, reflecting the high and low molar mass of these molecules, respectively. The thickest layers occurred for a concentration of 1.2 mg ml^{-1}, which is above the overlap concentration for all NaHA (Tadmor et al. 2002). Overall thickness ranged from 41 to 122 nm.

Atomic Force Microscopy

AFM contact force measurements and surface morphology images were obtained using a Digital Instruments Multimode Scanning Probe Microscope equipped with a Veeco fluid imaging cell and Veeco model NP-S10 tips. Tips were etched using a piranha solution before data collection. Contact force measurements were made using contact mode to determine the nominal contact force of the tip to the sample, $F = k\Delta Z$, where ΔZ is distance from the control point to Vcs_{min} and k is the spring constant, 0.32 N m^{-1} (Digital Instruments Veeco Metrology Group 1999). Force measurements were taken in 5 different spots per sample and the ΔZ values were averaged. The sensitivity representing the cantilever deflection signal versus voltage applied to the piezo was calibrated before measurement. Results of the contact force measurements appear in Figure 3.

The data demonstrate that human NaHa yielded the highest contact force, whereas contact force was nearly indistinguishable between the rooster comb and streptococcus zooepidemicus species over the range of concentrations tested. As shown in Figure 2, the human NaHA also produced the thickest films consistent with deeper penetration of the tip necessitating greater pull out force. The insensitivity to film thickness difference between rooster and streptococcus zooepidemicus NaHA layers suggests that film thickness is not the lone determinant (e.g., molecular weight of grafted chains). The contact force was essentially equal for all three species at a concentration of 1.2 mg ml^{-1}. Based on this result and the results in Figure 2 indicating an intermediate thickness value for rooster comb NaHA, we selected this particular NaHA concentration of 1.2 mg ml^{-1} for making grafted surfaces to investigate protein adsorption characteristics. Further analysis including surface topography and wettability were carried out on these NaHA coatings as a function of solution concentration. X-ray photoelectron spectroscopy (XPS) and zeta potential measurements were performed on the surface types used for the protein adsorption analysis.

Topographical and flattened images of the three types of hyaluronized surfaces were captured using AFM in the fluid tapping mode at a height of 30 nm. The surface roughness was determined as $RA=\frac{1}{n}\sum_{i-1}^{n}|Z_j|$, the arithmetic average of the absolute values of the surface height deviations measured from the mean plane, and $RMS=\sqrt{\sum_{i-1}^{n}|Z_j|/n}$, or root mean square measure of the average of the height deviations taken from the mean data plane. The software package Nanoscope III, version 5.12r2 was used to analyze the 500 nm scan size for each image. The ranges of values for RA roughness were 1.2–6.1 nm (human NaHA), 0.3–4.7 nm (rooster comb NaHA) and 0.2–3.2 nm (streptococcus zooepidemicus NaHA) whereas the ranges of values for RMS roughness were 1.6–7.4 nm (human NaHA), 0.5–7.4 nm (rooster comb NaHA) and 0.3–5.7 nm (streptococcus zooepidemicus NaHA). Although these roughness values showed no discernible trend with bulk concentration, they are consistent in magnitude with the measured persistence length of NaHA, 4.5 to 9 nm (Tadmor et al. 2002).

As an example, representative AFM images are demonstrated in Figure 4 for four different concentrations of rooster comb NaHA, including 0.5 mg ml^{-1}, which is below the overlap concentration, and 1.2, 2.0 and 3.4 mg ml^{-1} which encompass the semidilute regime and the concentration of NaHA in synovial fluid (3.4 mg ml^{-1}). At 1.2 mg ml^{-1} there is an inversion on the surface, seen on the topographic AFM, from brown to yellow. This suggests that the surface is completely covered by NaHA and a thicker layer denoted by surface features is observed. Similar features were noted for both the human NaHA and streptococcus zooepidemicus NaHA coated surfaces, which are not shown.

Figure 5 quantifies the dimensions of the surface features, such as those shown in Fig. 4. The diameter ranges from 21.8 to 188.6 nm for all specimens studied while the height ranges from 3.2–17.8 nm for all specimens examined. The diameters are not corrected for tip deconvolution and therefore the actual size is less than those reported. While the height and diameter features appear more or less uniform across the concentration spectrum for streptococcus zooepidemicus NaHA, the general trend is for the diameter and height sizes of the human NaHA and rooster comb NaHA to fluctuate in parallel below 1.2 mg ml^{-1} (height and width increase and decrease together with increasing concentration) and to fluctuate inversely above this concentration. In particular, at 3.4 mg ml^{-1}, the surface becomes rather smooth as noted by the flat pancake like features shown in Figure 4D. Similar surface structure is also observed for the human NaHA and streptococcus zooepidemicus NaHA surfaces at this highest concentration evaluated. Although quite small, these features are on the size scale of adsorbed proteins and therefore their existence must be identified and characterized for any future investigation to fully interpret the protein resistance associated with such surfaces.

X-ray photoelectron spectroscopy characterization

The surfaces were also evaluated for confirmation of dextran and HA immobilization using XPS with a Physical Electronics Quantum 2000 spectrometer with a 200 μm spot size and monochromatic Al Kα radiation (1486.68 eV). The X-ray source was operated at 50 W and 15 kV. Core-level signals were obtained at photoelectron takeoff angles of 45° (2.5 nm detection depths) with respect to the sample surface.

For dextranized silicon surfaces, XPS multiplex surveys showed the ratio of C to N on average to be 11.1. Our experiments yield a C to N ratio of 7.6 for the APTES layer, i.e., the aminated silicon. This is consistent with values ranging from 5.5 to 10.8 as appear in the literature, depending on the extent of hydrolysis (Howarter and Youngblood 2006). Since the dextran layer thickness can vary, detection of nitrogen from within the APTES layer is possible. The amine groups may be exposed within the dextran layer, since the AFM images as seen, for instance, in (Tsai et al. 2011a) for surfaces prepared identically can appear patchy. For our hyaluronized silicon surfaces made at the NaHA concentration of 1.2 mg ml^{-1}, XPS used under the same conditions as for dextran showed the ratio of C to N on average to be 10.8 (streptococcus zooepidemicus NaHA), 11.2 (human NaHA), and 11.4 (rooster comb NaHA). These values are all consistent with XPS results for HA films determined in chemisorptions experiments (D'Sa et al. 2011; Suh et al. 2005). Given that the ellipsometric data presented in Figure 2 indicate the HA films to be much thicker than the 2.5 nm detection depth used, it is unlikely that these measurements include interference from other chemical constituents present.

Zeta potential measurements

The zeta-potential of single side flat surface samples was measured using a DelsaNano-C zeta potential and submicron particle size analyzer (Beckmann Coulter) utilizing the flat surface cell. The electrophoretic mobility of probe particles between the flat surface samples and cell surface was measured by using electrophoretic light scattering. The zeta potential in volts (ξ) was calculated from the Smoluchowski equation:

$$\xi = k\frac{\pi\eta}{\varepsilon}U,$$

in which η is the viscosity of the solution at 25 °C, ε is the dielectric constant of the solution at 25 °C and U is the electrophoretic mobility of probe particles. The solution (10^{-3} M NaCl solution (40 ml) with probe particles (140 μl), pH = 7.01) was used in all measurements.

Each measurement was the average of 70 individual measurements performed at various positions (10 measurements each in 7 positions). All measurements were performed using at least three distinct surface samples. The technique was applied knowing that assessment of neutral molecules (e.g., dextran) is difficult to achieve using electrophoretic techniques.

For HA, the zeta potential measurements were independent of the various HA subtypes ($\xi = -11.8 \pm 3.4$ mV), indicating that the carboxylic acid functional groups of the HA layers confer a net negative surface charge. Zeta potential measurements of the dextranized surfaces were attempted, however the values obtained were not reproducible and varied between −100 and 100 mV. This phenomenon results from our preparation method for dextranized surfaces, which involves the oxidation of dextran using sodium periodate to prepare dialdehydes that covalently bind to the aminated surfaces. The resulting dextranized surfaces contain alcohols and aldehydes that do not ionize appreciably at physiologic pH (Hardwick 2007). Therefore, zeta potential measurements, which rely on flowing charged particles over the surface, were unable to determine reliably the surface charge of the nearly neutral dextranized surfaces.

Differential Quantification of Protein Adsorption

We prepared protein solutions and measured protein adsorption on the various silicon, dextran and NaHA surface subtypes using the experimental method detailed previously (Ombelli et al. 2005). Briefly, single and mixed solutions of BSA and Fg were prepared using 40 mM phosphate-buffer saline (PBS) at pH 7.0. Analytical grade chemicals for the buffer preparation were used without further purification. For these studies we restricted our choice of surfaces to six preparations: bare silicon, dextranized (0.5 hr and 4 hr oxidation time) and human NaHA, rooster comb NaHA and streptococcus zooepidemicus NaHA at 1.2 mg ml^{-1} concentration.

Proteins were adsorbed on surfaces by immersing various samples in protein-laden PBS solution containing a 50/50 mixture of BSA and Fg at concentrations of 20 and 40 μg ml^{-1} each for prescribed intervals of 10, 30, 60 or 120 min. Surfaces were rinsed with PBS to remove loosely bound proteins. The residual adsorbed proteins were eluted from the surfaces by immersion in 8 mM CHAPS solution on a shaker. Eluted protein samples were dialyzed in PBS to remove the CHAPS. Samples were frozen and then freeze-dried. The desorbed proteins were then identified and quantified using a Beckman Coulter System Gold® HPLC system running 32 Karat™ software to perform size exclusion chromatography. A detailed description of each step of the procedure is described elsewhere (Ombelli et al. 2005). All experiments were run in triplicate, with the mean values and standard deviations determined from the resultant measurements.

The elution spectra of single protein and binary 50/50 mixtures of BSA and Fg over a range of concentrations are shown in Figure 6, with data plotted with arbitrary magnitude as absorbance at 210 nm (A_{210}) versus retention time (min). This comparison allows unique and distinct identification of the two main peaks appearing at 11.9 min and 16.5 min for Fg (340 kDa) and BSA (66 kDa), respectively and provides calibration for the quantitative assessment of protein adsorption. Overall, the technique requires 24–36 hr from surface immersion in protein solution to completion of the quantitative analysis, which is sufficiently sensitive to detect nanogram amounts of protein. Protein recovery is nearly complete (Ombelli et al. 2005): a few additional experiments were conducted using fluorescently labeled proteins (Texas-Red tagged albumin and Oregon-Green tagged fibrinogen) to demonstrate that any residual protein remaining on the study surfaces following elution or on transfer surfaces such as the dialysis membrane was below the detection limit.

Contact Angle Measurement

Using a 2 μl sessile drop, water contact angle measurements were performed on bare, dextranized and hyaluronized surfaces before and after protein adsorption. Samples were not conditioned prior to measurements being made. For the protein cases, samples were immersed for 1 h in either single or double protein solutions at concentrations of 20 μg ml^{-1} in PBS. All measurements were made under ambient conditions with relative humidity ~50%. The analysis was performed using a Ramé-Hart (Mountain Lakes, NJ) model 100-00 goniometer with a software-controlled auto-pipetting system and the DROPimage advanced software package. Determination of the contact angle was by numerical curve fitting of the droplet profile at the three-phase boundary from the image captured by a CCD camera. Data were collected 1 to 2 s after the drop was deposited on the sample. Measurements were averaged for at least three drops on at least three different regions for each sample, with a minimum of five samples for each of the different surface coating.

Results and Discussion

The silicon wafers we have selected to use here as model materials are different from the silicones (e.g., PDMS and similar polymers) commonly used in medical devices such as tubing sets and catheters. Additionally, the amino-functionalization via silanization route we have taken for the dextran chemical surface modification is generally regarded as safe in terms of potential mutagenicity and toxicity when contact with the human body is anticipated. The grafted dextran and HA layers are stable, with AFM and ellipsometric evaluation of samples showing no degradation in surface features several weeks after synthesis.

The contact angle measurements on silicon, dextran grafted silicon and NaHA grafted silicon are given in Table 1. First, the NaHA surface has the lowest contact angle with water (most wettable). Second, exposure of dextranized surfaces to the salts from PBS lowers the contact angle by ~ 6° from the mean values obtained without PBS exposure. This effect was minimal on the hyaluronized surfaces. Third, surfaces covered with protein have a greater contact angle than untreated samples. Moreover, the contact angle values are confined to a narrow range of values for each surface. The largest contact angle of ~70° is found on the silicon wafer and the lowest contact angle of ~40° occurs on the hyaluronized surfaces. The contact angle measurements demonstrate relative equivalence for the specific subtypes of NaHA studied.

Figure 7 shows the surface density (Γ) of BSA (Figure 7A), Fg (Figure 7B) and total protein (Figure 7C) adsorbed from 50/50 mixed solutions at 20 μg ml^{-1} for each protein onto silicon, dextran- and hyaluronate-modified silicon. As seen in Figure 7A, after incubation for 10 min, the surface coverage of BSA ranged from a low of 3 ± 0.5 ng cm^{-2} on rooster comb and streptococcus zooepidemicus hyaluronate-coated silicon to a high of 29 ± 2 ng cm^{-2} on silicon, with the intermediate coverage of 7 ± 1 ng cm^{-2} and 16 ± 1 ng cm^{-2} found for the two dextran-coated silicon surfaces having 0.5 h and 4 h oxidation times, respectively. This rank order of $\Gamma_{Si} > \Gamma_{Dex} > \Gamma_{HA}$ was maintained for BSA coverage for each of the longer exposure times. BSA coverage approached a constant value after 60 min for all substrate types. Compared to the 10 min values, the BSA coverage increased 10 to 17-fold on the hyaluronate-coated silicon, 12-fold on the 0.5 h dextran-coated silicon, 14-fold on the 4 h dextran-coated silicon and 12-fold on the silicon surface, which adsorbed a maximum of 358 ± 11 ng cm^{-2}.

As seen in Figure 7B, after incubation for 10 min, the values of the surface coverage of Fg were tightly clustered in the range of 5–10 ng cm^{-2} for the three different subtypes of hyaluronate coatings and both the 0.5 h and 4 h dextran-coated silicon. Protein adsorption

was noticeably greater on silicon (46 ± 4 ng cm^{-2}), even at this early time point. At times sufficiently long for adsorption to have reached a plateau on all surfaces, the rank order for Fg coverage was $\Gamma_{Si} > \Gamma_{Dex\_4hr} = \Gamma_{HA} > \Gamma_{Dex\_0.5hr}$. Maximal coverage was observed to occur by 30 min for the 0.5 h dextran-coated silicon and at 1 hr for the other surfaces. At maximal coverage the Fg surface concentrations were 22 ± 2 ng cm^{-2} on 0.5 h dextran-coated silicon, in the range of 35 ± 3 to 42 ± 3 ng cm^{-2} for the three different NaHA coatings as well as 4 h dextran-coated silicon and 103 ± 7 ng cm^{-2} on bare silicon. Overall, the total surface coverage (BSA + Fg) seen in Figure 7C follows the trend for BSA surface coverage represented in Figure 7A, with $\Gamma_{Si} > \Gamma_{Dex\_4hr} > \Gamma_{Dex\_0.5hr} = \Gamma_{HA}$ throughout, with tight clustering of the values for the three NaHA subtypes and the 0.5 h dextranized surfaces. At maximal coverage, occurring at 1 h or longer, the total protein surface concentration was 461 ± 41 ng cm^{-2} on silicon, 262 ± 17 ng cm^{-2} on 4 h dextran-coated silicon, and in the range of 83 ± 8 to 106 ± 13 ng cm^{-2} for the three NaHA subtypes and the 0.5 h dextranized surfaces, all of which were closely grouped.. These findings demonstrate that, with respect to bare silicon surfaces, the polysaccharide coatings reduce the maximum total protein coverage by 43% for 4 h dextranized silicon, by 77 to 82% for the 0.5 h dextranized silicon the three different hyaluronized silicon surfaces. Moreover, after 1 h of protein exposure, all surfaces showed preferential adsorption of BSA from the mixed BSA/Fg solution, with the percentage of BSA ranging from 56 to 58% of the total protein adsorbed on the various hyaluronate-coated silicon surfaces, 78% (bare silicon) and 79 to 85% on the various dextran-coated silicon surfaces. This result indicates some surface-based specificity for the differential competitive adsorption of the proteins.

Results for the experiments conducted using the higher protein concentrations of 40 μg ml^{-1} appear in Figure 8. As before, the maximum surface coverage was also achieved at the 1 h time point for these experiments. The effect of increasing the BSA concentration in the bulk liquid had its greatest influence on surface coverage of silicon at short (10–30 min) time, with surface concentrations being ~ 2–3 times higher than those found with the lower bulk concentration (Figure 7A). At long times (1 h or more), however, the BSA surface coverage was only ~ 10% higher than was found using the lower bulk concentration. The effect of increasing the BSA concentration in the bulk liquid also influenced the surface coverage of the dextranized surfaces at short (10 min) time, with surface concentrations being ~ 2.4 times higher than those found with the lower bulk concentration (Figure 7A). At longer times (30 min or more), however, the BSA surface coverage was ~ 50% higher on the dextranized surfaces and approximately doubled on each of the hyaluronized surface subtypes than was found using the lower bulk concentration. While this may speak to some surface specificity for competitive adsorption between the different proteins, it also points to maximal surface coverage with albumin occurring. A monolayer covering has been reached at the lower concentration, and this is followed by the formation of protein multilayers as observed in (Holmberg and Hou 2010) with the bulk concentration having been increased.

As indicated in Figure 8B, the effect of increasing the Fg concentration was much more pronounced on the silicon surfaces compared to the dextranized surfaces, especially after sufficient time for maximum surface concentration to be achieved. The Fg surface concentration was ~4.4-fold higher than was measured on surfaces following exposure to the lower bulk concentration. The dextranized surfaces more fully resisted additional Fg adsorption at the higher bulk protein concentration, with maximal surface concentration being 90 ± 7 ng cm^{-2} and 26 ± 2 ng cm^{-2} for the 4h and 0.5 h dextran preparations, respectively. For the 0.5 h dextranized surface, this represented an increase of only ~18% from the surface concentration maximum measured after sample immersion in the lower bulk concentration solution. Each of the three subtype hyaluronized surfaces strongly resisted biofouling with Fg, similar to the 0.5 h dextranized surface, across the entire time domain. Under conditions of higher bulk protein concentrations, the Fg surface

concentrations fell from higher values (Figure 7B) to values in the range of 18 ± 1 to 25 ± 2 ng cm^{-2} for these experiments. These surface concentrations are actually 29–40% lower than were found with the 20 μg ml^{-1} bulk protein solution. In the face of a net increase in the total protein adsorption occurring (Figure 8C) in comparison to that occurring at the lower bulk concentration (Figure 7C), there is a greater resistance to Fg adsorption, or, alternatively, a competitive advantage for BSA adsorption, to these particular surfaces at the higher bulk protein concentration.

Similar findings have been observed by Holmberg et al. (Holmberg and Hou 2010) for competitive adsorption of albumin and fibrinogen onto polyethylene terephthalate and glass surfaces. Their work demonstrates not only that albumin forms multilayers on the surface, but that the interface region acts as a disordered matrix of different proteins in which the various species can have surface interactions, interactions with other proteins, or interactions that involve both the surface and other proteins. The resultant magnitude of protein adsorption is dependent on the nature and strength of interactions. Conceptually, proteins are able to adsorb into multiple layers stacked atop each other. Moreover, the replacement of high mobility proteins that arrive to the surface early by less motile proteins which bear a higher affinity for the surface (i.e., the Vroman effect) is dependent on fibrinogen levels. While this does not have to be the dominant process during competitive adsorption, the decrease in fibrinogen levels observed in the face of increased fibrinogen levels raises the possibility that albumin may have a higher affinity for certain surfaces and thereby resist competition with, or replacement by, fibrinogen.

The total protein surface concentration again tracked directly with the BSA concentration, as shown in Figure 8C. It is important to note that doubling the bulk BSA and Fg concentrations yielded nearly a doubling of the maximal total protein surface concentration on the silicon surfaces at long times, from 461 ± 41 ng cm^{-2} (Figure 7C) to 849 ± 47 ng cm^{-2}. This was about 5.5 to 6 times greater than the total protein surface concentration (Figure 7C) measured at long times on all three types of hyaluronized surfaces and the 0.5 h dextranized surfaces. The effect of doubling the bulk protein concentrations was to increase the total protein surface concentration measured at long times by ~45% on each of the two different dextranized surfaces and, differentially, by 45% for human NaHA, 60% for rooster comb NaHA and by 84% for streptococcus zooepidemicus NaHA. While it may appear coincidental that the two proteins reached maximal surface coverage at approximately the same time, this is likely to result from our selection of bulk concentrations lower than levels often studied (Holmberg and Hou 2010; Oesterberg et al. 1995), diffusion limited transport processes for the proteins out of the bulk solution (Lampe et al. 2010).

The differences in protein adsorption onto the various surface coatings we have tested are characteristically related to surface structure. We have previously prepared and characterized thin hydrated dextran films on silanized substrates (Miksa et al. 2004; Miksa et al. 2006; Ombelli et al. 2002; Ombelli et al. 2003; Ombelli et al. 2005), with the resultant properties of dextranized films prepared by our method to be in agreement with those prepared by other investigators (Beyer et al. 1996; Kuhner and Sackmann 1996). Our hyaluronized surfaces are newly evaluated both for surface structure as well as for protein coverage. These surfaces have been optimized for the protein adsorption experiments by selecting a specific bulk concentration (1.2 mg ml^{-1}) from a wide array of possibilities examined in our preliminary characterization work. However, based on AFM results obtained and presented in Figures 3, 4 and 5, along with the surface roughness results (above) and wetting data (Table 1), our choice of a single bulk NaHA concentration for synthesis of surfaces for the more advanced studies of protein adsorption yields a cohesive set of similar data for each of the three types of hyaluronate examined. Interestingly, the dimensional characteristics of the features present on these new surfaces has been shown to

have yielded the tallest structures bearing the smallest diameters of all of the surface features examined over the range of concentrations studied, as shown in Figure 5. One might think that such a detailed surface structure would present an enormous surface area for protein adsorption. However the various hyaluronized surfaces, despite their intrinsically distinct morphological features and unique biological derivations, were nonetheless equally resistant to total protein adsorption while not being substantially different from the 0.5 h dextranized surfaces in this regard.

While the improved resistance to protein adsorption of NaHa and 0.5 h dextran compared to the 4 h dextran and bare silicon might appear consistent with the water contact angle measurements in Table 1, other studies of anti-fouling coatings have shown that there is no direct relationship between the value of the water contact angle and protein deposition on the surface layer (Emmenegger et al. 2009). We have performed these experiments at a physiological value of pH and using a balanced salt solution. This has the effect of maintaining meaningful, electrostatic interactions between elements of the surface coatings, and the proteins to which the surfaces are exposed consistent with the biological milieu in which vascular devices are employed. Extremes of pH and salt concentration are known to cause significant deviation in the electrostatic interactions involved in biofouling (Su and Li 2007). Additionally, the specific chemical composition, the roughness, and the topography all contribute to the affinity of plasma proteins as biofouling occurs. However, the direct into relationships between the physical and chemical properties of surfaces in the protein adsorption responses they elicit are not fully understood. Therefore, the ability to craft tailor made surfaces to control space biofouling still relies on experimental methods aimed at discerning the structure/function relationships. Certainly, important biological processes such as protein adsorption are controllable to some degree. Using chemical grafting methods such as those employed here to induce surface modifications onto soft materials gives rise to the possibility that biomimetic function, or at least bioinert characteristics, can be imparted in a scalable manufacturing process (Variola et al. 2009).

Differential effects of the surface coatings on both total and individual protein adsorption most likely result from the chemical composition of the surface coatings, as well as their topology. Both fibrinogen (Cai et al. 2006) and albumin (Xiang D.Z. et al. 2007) have been shown to adsorb less to those surfaces having lower zeta potential. Our findings for HA coated surfaces, for which the zeta potential is negative, are consistent in this regard, as demonstrated in Figures 7 and 8. However, the proteins studied do not necessarily adsorb with greater mass per area to the dextran coatings, which bear a relatively neutral surface charge. We have also shown in Figures 7 and 8 that the oxidation time used in the preparation of dextranized surfaces translates directly into effects on biofouling. Dextran, a naturally occurring polysaccharide, has many characteristics that are favorable for its application as an anti-fouling coating. It is water soluble, neutral, and non-toxic. One recent evaluation of the protein resistance of dextranized surfaces clearly demonstrated that both the molecular weight, and the relative degree of oxidation markedly influenced both the chemical structure of the surface molecules, and the degree to which they resisted protein adsorption (Martwiset et al. 2006). Our finding that surface saturation with protein has occurred by one hour is consistent with experimental technique used in those experiments.

The protein repelling capability of our hyaluronate coated surfaces is consistent with that demonstrated by a variety of graft copolymers bearing dextran side chains (Perrino et al. 2008). The rationale in those studies was to mimic biological membrane surfaces through the use of a biomimetic alternative to the highly hydrated glycocalyx cell coating known for its anti-adhesive properties. This is particularly important in preventing blood clotting in response to its contact with artificial surfaces (Keuren et al. 2003). Our rationale is similar in that the biologic interface between blood and the vasculature is the endothelial cell

glycocalyx. In addition to carbohydrates, its molecular structure is comprised by significant fraction of glycoproteins and proteoglycans and includes hyaluronic acid as a major backbone molecule. Thus, sodium hyaluronate is an accessible compound that may therefore serve as an acceptable biology-inspired alternative to dextran as a component of an antifouling surface coating. HA-based hydrogels have been shown to have anti-adhesive properties for cell adhesion. Park et al. (Park et al. 2003) found that fibroblasts did not spread on HA-containing gel surfaces. Polystyrene surfaces modified via immobilization of hyaluronic acid have been shown to resist attachment of human lens epithelial cells for application in ocular medicine (D'Sa et al. 2011). Patterned surfaces of dextran and HA show preferential attachment of macrophages to the dextranized regions (Tsai et al. 2011b). In contrast to cell binding resistance, some HA materials have been shown to enhance bacterial adhesion, and HA modified PDMS surfaces were recently shown to enhance corneal epithelial cell and 3T3 fibroblast adhesion (Alauzun et al. 2010). These examples indicate that resistance to, or enhancement of, adhesion of specific cell lines may depend on the presence of HA molecules in the surface layer.

The physical immobilization of hyaluronic acid in the model hydrogels has previously been shown to reduce protein adsorption. Suh et al. (Suh et al. 2005) showed HA applied by spin coating onto glass resulted in reductions in BSA, fibronectin and IgG adhesion. Van Beek et al. (Van Beek et al. 2008) studied protein adsorption onto HA containing hydrogels. Although their specific application was for contact lenses, and the fact that the associated study protein, lysozyme, is not considered to be a significant offender in blood plasma-based biofouling, the study does indicate an influence of a high-density hydrated interfacial layer to overcome charge effects governing protein adherence to the surface. Our results, bolstered by the zeta potential measurements, are certainly consistent with this approach. We add also to the understanding of this effect by our study of the differential effects of multiple hyaluronic acids (i.e., human, rooster comb, streptococcus zooepidemicus) as well as two distinct dextran preparations in this project.

This study also demonstrates a major advantage of our CHAPS/HPLC experimental technique to measure the protein surface concentration, since the approach is both quantitative and selective. This method enables us to interrogate competitive protein adsorption to biomaterials, especially vascular implants and other blood-contacting surfaces without having to rely on indirect methods such as protein depletion from the bulk liquid phase (Noh and Vogler 2006) or X-ray photoelectron spectroscopy (XPS) (Hamilton-Brown et al. 2009; Morra and Cassinelli 1998; Su and Li 2007). While our method was originally tested using bare silicon and dextran-grafted silicon surfaces synthesized and characterized in our laboratories (Miksa et al. 2004; Ombelli et al. 2002; Ombelli et al. 2003), it has proven to be equally useful for the hyaluronized surfaces studied.

Conclusion

Biofouling of coated surfaces in contact with plasma proteins occurs rapidly but is differentially dependent both on surface molecular structure and the protein concentration to which the surfaces are exposed. Concurrent albumin and fibrinogen adsorption from a binary solution measured by the CHAPS/HPLC method increase monotonically to saturation on bare, dextranized and hyaluronized silicon surfaces. As expected, the degree of dextran oxidation correlates with the extent of protein adsorption. Total protein coverage on the hyaluronized surface was comparable to that for the 0.5 h oxidized dextran coating. This was approximately an order of magnitude smaller than the protein coverage on bare silicon. Aqueous AFM imaging afforded us the height, diameter, and roughness of the hyaluronate surfaces, enabling us to choose a consistent surface preparation across the three different species derivations in the semi-dilute regime. The water contact angle data indicate the

hyaluronate coatings to be more hydrophilic than the dextranized surfaces, although the surface topology is comparably dimensioned. This study reveals that the molecular structure and molecular composition of a surface coating remain fundamental variants in its biofouling potential. Additionally, for the hyaluronized surfaces, increasing the bulk concentration of the proteins led to a reduction in the surface biofouling with fibrinogen at the expense of an increase in albumin surface coverage. This may have implications for biocompatibility in terms of resultant immune responses, cellular adhesion and thrombogenesis in a more replete biological environment. Overall, surface coating by hyaluronization provides a biological molecule alternative to dextran for the synthesis of a thin film layer comprised of a molecular constituent of the endothelial cell glycocalyx. Based on the protein adsorption measurements presented, surface grafting of a hyaluronate layer affords significant antifouling capability.

Acknowledgments

We are grateful to the NIH for support through grant R01 HL60230 (DME). Partial support was provided by the NSF Polymers (DMR05-49307), MRSEC (DMR05-20020) and NSEC (DMR04-25780) programs (LC, RJC). Thanks to Hyun-Su Lee and Daeyeon Lee for their assistance with zeta potential measurements. We appreciate Thomas P. Russell and Jack Hirsch (Materials Research Science and Engineering Center at University of Massachusetts) for XPS measurements.

References

Alauzun JG, Young S, D'Souza R, Liu L, Brook MA, Sheardown HD. Biocompatible, hyaluronic acid modified silicone elastomers. Biomaterials. 2010; 31:3471–3478. [PubMed: 20138660]

Babensee JE, Cornelius RM, Brash JL, Sefton MV. Immunoblot analysis of proteins associated with HEMA-MMA microcapsules: Human serum proteins in vitro and rat proteins following implantation. Biomaterials. 1998; 19:839–849. [PubMed: 9663761]

Beyer D, Knoll W, Ringsdorf H, Elender G, Sackmann E. Covalently attached polymer mono- and multilayers on silanized glass substrates. Thin Solid Films. 1996; 284–285:825–828.

Cai K, Frant M, Bossert J, Hildebrand G, Liefeith K, Jandt KD. Surface functionalized titanium thin films: Zeta-potential, protein adsorption and cell proliferation. Colloids Surf B Biointerfaces. 2006; 50:1–8. [PubMed: 16679008]

Castner DG, Ratner BD. Biomedical surface science: Foundations to frontiers. Surf Sci. 2002; 500:28–60.

Cornelius RM, Brash JL. Adsorption from plasma and buffer of single- and two-chain high molecular weight kininogen to glass and sulfonated polyurethane surfaces. Biomaterials. 1999; 20:341–350. [PubMed: 10048406]

Cornelius RM, Sanchez J, Olsson P, Brash JL. Interactions of antithrombin and proteins in the plasma contact activation system with immobilized functional heparin. J Biomed Mater Res A. 2003; 67A: 475–483. [PubMed: 14566788]

Cryer, A. Biochemical interactions at the endothelium. New York: Elsevier; 1983.

D'Sa RA, Dickinson PJ, Raj J, Pierscionek BK, Meenan BJ. Inhibition of lens epithelial cell growth via immobilisation of hyaluronic acid on atmospheric pressure plasma modified polystyrene. Soft Matter. 2011; 7:608–617.

Dai L, StJohn HAW, Bi J, Zientek P, Chatelier RC, Griesser HJ. Biomedical coatings by the covalent immobilization of polysaccharides onto gas-plasma-activated polymer surfaces. Surf Interface Anal. 2000; 29:46–55.

Dejardin P, ten Hove P, Yu XJ, Brash JL. Competitive adsorption of high molecular weight kininogen and fibrinogen from binary mixtures to glass surface. Langmuir. 1995; 11:4001–4007.

Digital Instruments Veeco Metrology Group. MultiModeTM SPM Instruction Manual. 1999

Edmunds, LH., Jr.; Hessel, EA., II; Colman, RW.; Menasche, P.; Hammon, JW, Jr.. Extracorporeal Circulation. Second Edition. Vol. 11. McGraw-Hill Companies, Inc.; 2003. Cardiac Surgery In The Adult; p. 315-387.

Emmenegger CR, Brynda E, Riedel T, Sedlakova Z, Houska M, Alles AB. Interaction of blood plasma with antifouling surfaces. Langmuir. 2009; 25:6328–6333. [PubMed: 19408903]

Engel MFM, Visser AJWG, van Mierlo CPM. Refolding of adsorbed bovine a-Lactalbumin during surfactant induced displacement from a hydrophobic interface. Langmuir. 2003; 19:2929–2937.

Grunkemeier JM, Tsai WB, Horbett TA. Co-adsorbed fibrinogen and von Willebrand factor augment platelet procoagulant activity and spreading. J Biomat Sci-Polym E. 2001; 12:1–20.

Grunkemeier JM, Tsai WB, McFarland CD, Horbett TA. The effect of adsorbed fibrinogen, fibronectin, von Willebrand factor and vitronectin on the procoagulant state of adherent platelets. Biomaterials. 2000; 21:2243–2252. [PubMed: 11026630]

Hamilton-Brown P, Gengebach T, Griesser HJ, Meagher L. End terminal, poly(ethylene oxide) graft layers: surface forces and protein adsorption. Langmuir. 2009; 25:9149–9156. [PubMed: 19534458]

Hardwick, ERBJ. Introduction to Chemistry. Fort Worth: Harcourt College Publishers; 2007.

Hartley PG, McArthur SL, McLean KM, Griesser HJ. Physicochemical properties of polysaccharide coatings based on grafted multilayer assemblies. Langmuir. 2002; 18:2483–2494.

Holmberg M, Hou X. Fibrinogen adsorption on blocked surface of albumin. Colloids and Surfaces B: Biointerfaces. 2010; 84:71–75.

Horbett, TA.; Brash, JL. ACS Symposium Series 602, Proteins at Interfaces II Fundamentals and Applications. American Chemical Society; Washington, DC. 1995.

Howarter JA, Youngblood JP. Optimization of silica silanization by 3-aminopropyltriethoxysilane. Langmuir. 2006; 22:11142–11147. [PubMed: 17154595]

Jenney CR, Anderson JM. Adsorbed serum proteins responsible for surface dependent human macrophage behavior. J Biomed Mater Res. 2000; 49:435–447. [PubMed: 10602077]

Keuren JFW, Wielders SJH, Willems GM, Morra M, Cahalan L, Cahalan P, Lindhout T. Thrombogenicity of polysaccharide-coated surfaces. Biomaterials. 2003; 24:1917–1924. [PubMed: 12615482]

Kim J, Somorjai GA. Molecular packing of lysozyme, fibrinogen, and bovine serum albumin on hydrophilic and hydrophobic surfaces studied by infrared-visible sum frequency generation and fluorescence microscopy. J Am Chem Soc. 2003; 125:3150–3158. [PubMed: 12617683]

Klomp AJA, Engbers GHM, Mol J, Terlingen JGA, Feijen J. Adsorption of proteins from plasma at polyester non-wovens. Biomaterials. 1999; 20:1203–1211. [PubMed: 10395389]

Kuhner M, Sackmann E. Ultrathin hydrated dextran films grafted on glass: Preparation and characterization of structural, viscous, and elastic properties by quantitative microinterferometry. Langmuir. 1996; 12:4866–4876.

Lampe JW, Liao ZZ, Dmochowski IJ, Ayyaswamy PS, Eckmann DM. Imaging macromotecular interactions at an interface. Langmuir. 2010; 26:2452–2459. [PubMed: 20085337]

Lassen B, Malmsten M. Competitive protein adsorption studied with TIRF and ellipsometry. J Colloid Interf Sci. 1996a; 179:470–477.

Lassen B, Malmsten M. Structure of protein layers during competitive adsorption. J Colloid Interf Sci. 1996b; 180:339–349.

Lassen B, Malmsten M. Competitive protein adsorption at plasma polymer surfaces. J Colloid Interf Sci. 1997; 186:9–16.

Martins MCL, Wang D, Ji J, Feng L, Barbosa MA. Albumin and fibrinogen adsorption on PU-PHEMA surfaces. Biomaterials. 2003; 24:2067–2076. [PubMed: 12628827]

Martwiset S, Koh AE, Chen W. Nonfouling characteristics of dextran-containing surfaces. Langmuir. 2006; 22:8192–8196. [PubMed: 16952261]

Mason M, Vercruysse KP, Kirker KR, Frisch R, Marecak DM, Prestwich GD, Pitt WG. Attachment of hyaluronic acid to polypropylene, polystyrene, and polytetrafluoroethylene. Biomaterials. 2000; 21:31–36. [PubMed: 10619676]

Miksa, D.; Irish, ER.; Chen, D.; Composto, RJ.; Eckmann, DM. Biomimetic surfaces via dextran immobilization; characterization and analysis; Mat Res Soc Symp Proc; 2004. p. V2.2.1-V2.2.7.

Miksa D, Irish ER, Chen D, Composto RJ, Eckmann DM. Dextran functionalized surfaces via reductive amination: morphology, wetting, and adhesion. Biomacromolecules. 2006; 7:557–564. [PubMed: 16471930]

Morra M, Cassinelli C. Simple model for the XPS analysis of polysaccharide-coated surfaces. Surf Interface Anal. 1998; 26:742–747.

Noh H, Vogler EA. Volumetric interpretation of protein adsorption: Mass and energy balance for albumin adsorption to particulate adsorbents with incrementally increasing hydrophilicity. Biomaterials. 2006; 27:5801–5812. [PubMed: 16928398]

Oesterberg E, Bergstrom K, Holmberg K, Schuman TP, Riggs JA, Burns NL, Van Alstine JM, Harris JM. Protein-rejecting ability of surface-bound dextran in end-on and side-on configurations: comparison to PEG. J Biomed Mater Res. 1995; 29:741–747. [PubMed: 7593011]

Ombelli M, Composto RJ, Meng QC, Eckmann DM. A quantitative and selective chromatography method for determining coverages of multiple proteins on surfaces. J Chromatogr B Analyt Technol Biomed Life Sci. 2005; 826:198–205.

Ombelli, M.; Eckmann, DM.; Composto, RJ. Biomimetic dextran coatings on silicon wafers: Thin film properties and wetting; Mat Res Soc Symp Proc; 2002. p. 205-210.

Ombelli, M.; Eckmann, DM.; Composto, RJ. Dextran grafted silicon substrates: Preparation, characterization and biomedical applications; Mat Res Soc Symp Proc; 2003. p. 93-98.

Park YD, Tirelli N, Hubbell JA. Photopolymerized hyaluronic acid-based hydrogels and interpenetrating networks. Biomaterials. 2003; 24:893–900. [PubMed: 12504509]

Perrino C, Lee S, Choi SW, Maruyama A, Spencer ND. A biomimetic alternative to poly(ethylene glycol) as an antifouling coating: Resistance to nonspecific protein adsorption of poly(L-lysine)-graft-dextran. Langmuir. 2008; 24:8850–8856. [PubMed: 18616303]

Stile RA, Barber TA, Castner DG, Healy KE. Sequential robust design methodology and x-ray photoelectron spectroscopy to analyze the grafting of hyaluronic acid to glass substrates. J Biomed Mater Res. 2002; 61:391–398. [PubMed: 12115464]

Su YL, Li C. The reorientation of poly(2-dimethylamino ethyl methacrylate) after environment stimuli improves hydrophilicity and resistance of protein adsorption. J Colloid Interf Sci. 2007; 316:344–349.

Suh KY, Yang JM, Khademhosseini A, Berry D, Tran TNT, Park H, Langer R. Characterization of chemisorbed hyaluronic acid directly immobilized on solid substrates. J Biomed Mater Res. 2005; 72B:292–298.

Tadmor R, Chen NH, Israelachvili JN. Thin film rheology and lubricity of hyaluronic acid solutions at a normal physiological concentration. J Biomed Mater Res. 2002; 61:514–523. [PubMed: 12115441]

Toworfe GK, Composto RJ, Adams CS, Shapiro IM, Ducheyne P. Fibronectin adsorption on surface-activated poly(dimethylsiloxane) and its effect on cellular function. J Biomed Mater Res. 2004; 71A:449–461.

Tsai IY, Tomczyk N, Eckmann JI, Composto RJ, Eckmann DM. Human plasma protein adsorption onto dextranized surfaces: a two-dimensional electrophoresis and mass spectrometry study. Colloids Surf B Biointerfaces. 2011a; 84:241–252. [PubMed: 21277175]

Tsai IY, Tomczyk N, Stachelek SJ, Composto RJ, Eckmann DM. Human macrophage adhesion on polysaccharide patterned surfaces. Soft Matter. 2011b; 7:3599–3606. [PubMed: 21479122]

Tsai WB, Grunkemeier JM, Horbett TA. Human plasma fibrinogen adsorption and platelet adhesion to polystyrene. J Biomed Mater Res. 1999; 44:130–139. [PubMed: 10397913]

Tsai WB, Grunkemeier JM, McFarland CD, Horbett TA. Platelet adhesion to polystyrene-based surfaces preadsorbed with plasmas selectively depleted in fibrinogen, fibronectin, vitronectin, or von Willebrand's factor. J Biomed Mater Res. 2002; 60:348–359. [PubMed: 11920657]

Tsai WB, Horbett TA. The role of fibronectin in platelet adhesion to plasma preadsorbed polystyrene. J Biomat Sci-Polym E. 1999; 10:163–181.

Van Beek M, Weeks A, Jones L, Sheardown H. Immobilized hyaluronic acid containing model silicone hydrogels reduce protein adsorption. J Biomater Sci Polym Ed. 2008; 19:1425–1436. [PubMed: 18973721]

Variola F, Vetrone F, Richert L, Jedrzejowski P, Yi JH, Zalzal S, Clair S, Sarkissian A, Perepichka DF, Wuest JD, Rosei F, Nanci A. Improving biocompatibitity of implantable metals by nanoscale modification of surfaces: an overview of strategies, fabrication methods, and challenges. Small. 2009; 5:996–1006. [PubMed: 19360718]

Wagner MS, Horbett TA, Castner DG. Characterizing multicomponent adsorbed protein films using electron spectroscopy for chemical analysis, time-of-flight secondary ion mass spectrometry, and radiolabeling: capabilities and limitations. Biomaterials. 2003a; 24:1897–1908. [PubMed: 12615480]

Wagner MS, Shen M, Horbett TA, Castner DG. Quantitative analysis of binary adsorbed protein films by time of flight secondary ion mass spectrometry. J Biomed Mater Res A. 2003b; 64A:1–11.

Weber N, Wendel HP, Ziemer G. Hemocompatibility of heparin-coated surfaces and the role of selective plasma protein adsorption. Biomaterials. 2001; 23:429–439. [PubMed: 11761163]

Xiang DZ, Hong SF, Chen XN, Li DX, Zhang DZ. Contribution of surface charge to bovine serum albumin adsorption on hydroxyapatite ceramic particles. Key Engineering Materials. 2007; 330–332:861–864.

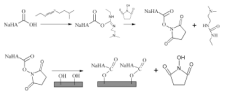

Figure 1.
Mechanism for surface immobilization of NaHA onto SiO_2 via the EDC/NHS method.

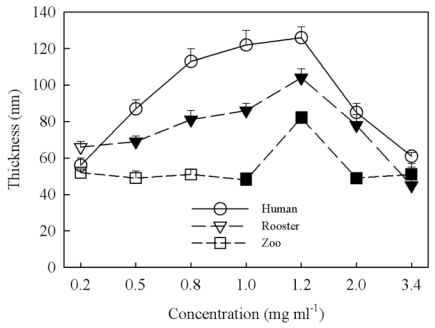

Figure 2.

Ellipsometric thickness (Å) of (●) human, (▽,▼) rooster comb and (□,■) streptococcus zooepidemicus NaHA grafted layers as a function of bulk substrate concentration during processing. Concentrations of NaHA in the dilute and semi-dilute regimes (i.e., below and above c*, the overlap concentration) for each specific species are delineated by open and solid symbols, respectively.

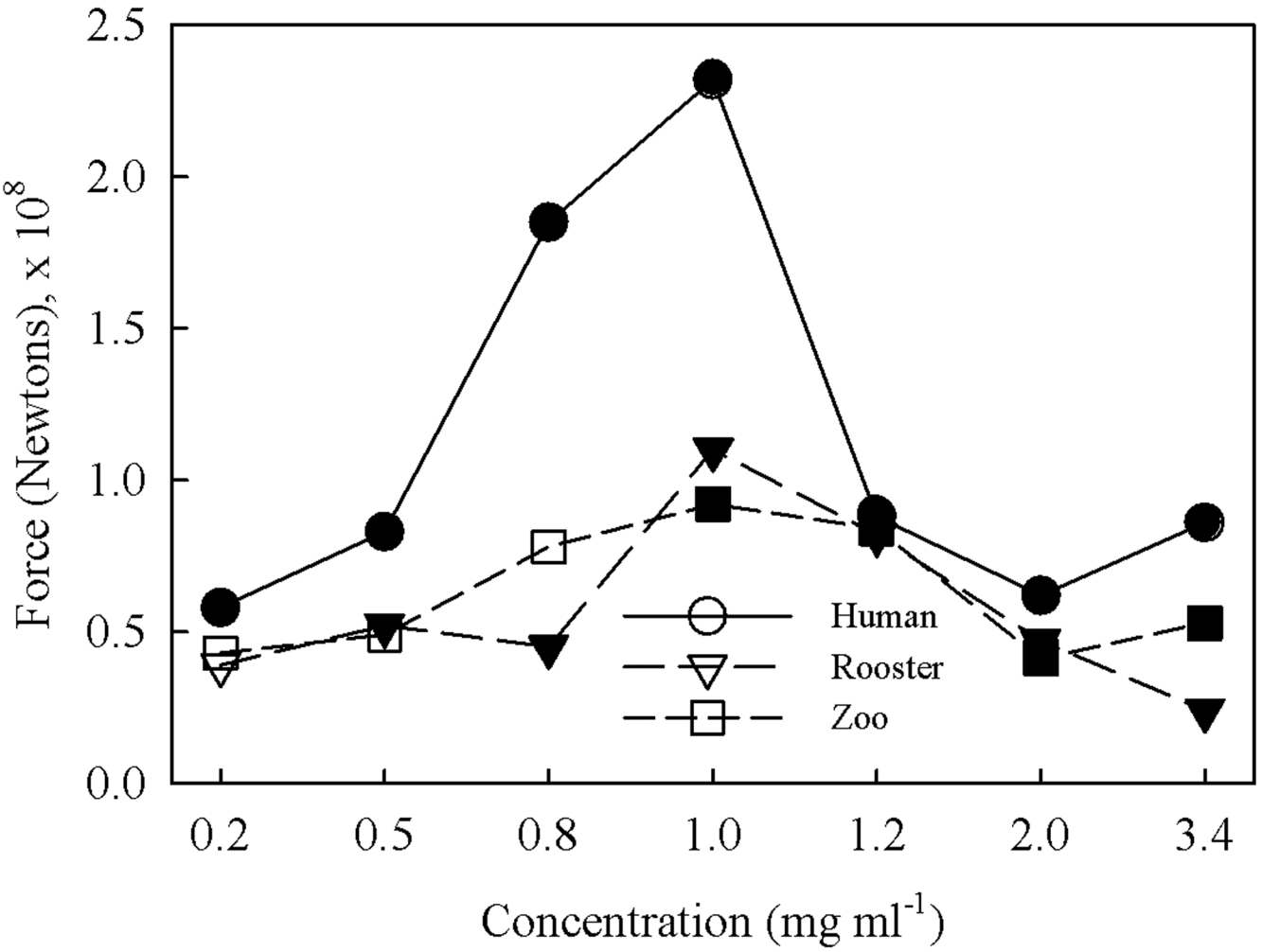

Figure 3.
Atomic Force Microscopy measurement of adhesion force of (●) human, (▽,▼) rooster comb and (□,■) streptococcus zooepidemicus NaHA grafted layers as a function of bulk substrate concentration during processing. Concentrations of NaHA in the dilute and semi-dilute regimes (i.e., below and above c*, the overlap concentration) for each specific species are delineated by open and solid symbols, respectively.

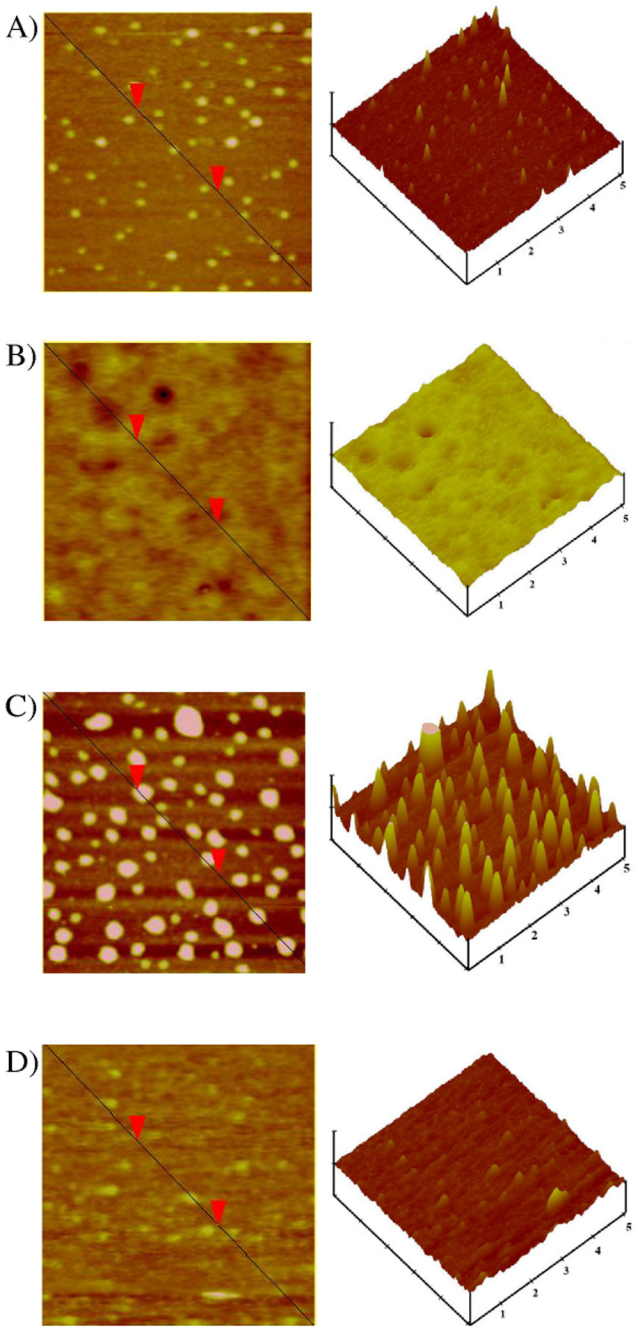

Figure 4.
Representative flattened and topographic AFM images of rooster comb NaHA at concentrations of A) 0.5 mg ml^{-1}, B) 1.2 mg ml^{-1}, C) 2.0 mg ml^{-1} and D) 3.4 mg ml^{-1}. Vertical scale 30 nm, scan size 500 nm.

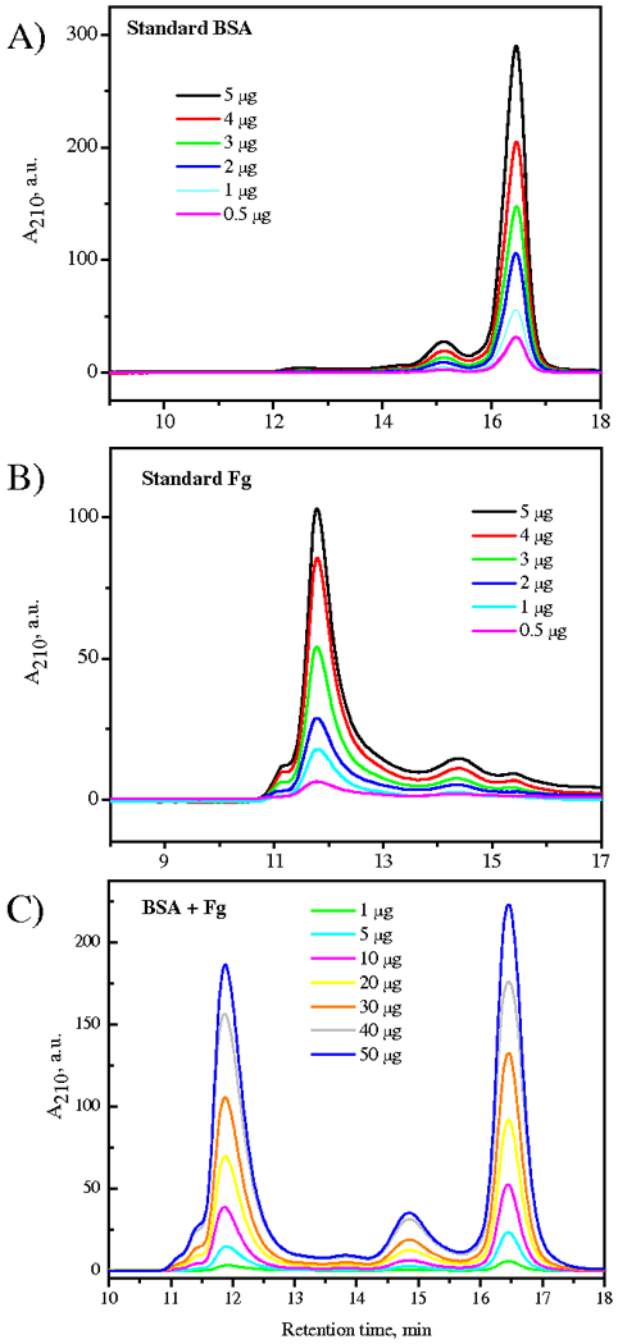

Figure 5.

Average feature height (□,■) and diameter (○,●) determined from topographic AFM images of human, rooster comb and streptococcus zooepidemicus NaHA grafted layers as a function of bulk substrate concentration during processing. Concentrations of NaHA in dilute and semi-dilute regime (i.e., below and above c*, the overlap concentration) are delineated by open and solid symbols, respectively.

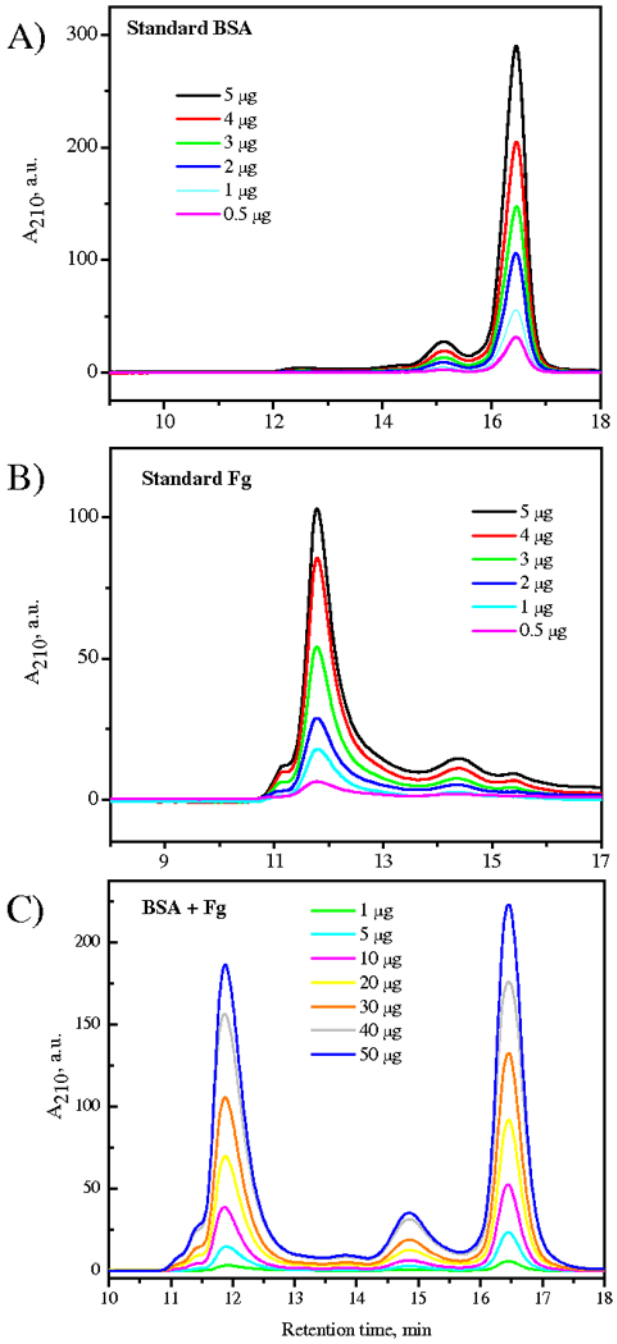

Figure 6.

Size exclusion chromatography analysis of single protein solutions of (A) BSA and (B) Fg over a 0.5–5 μg ml^{-1} range of concentrations and (c) of 50:50 binary protein solutions of BSA and Fg over a 1–50 μg ml^{-1} (total mass) range of concentrations.

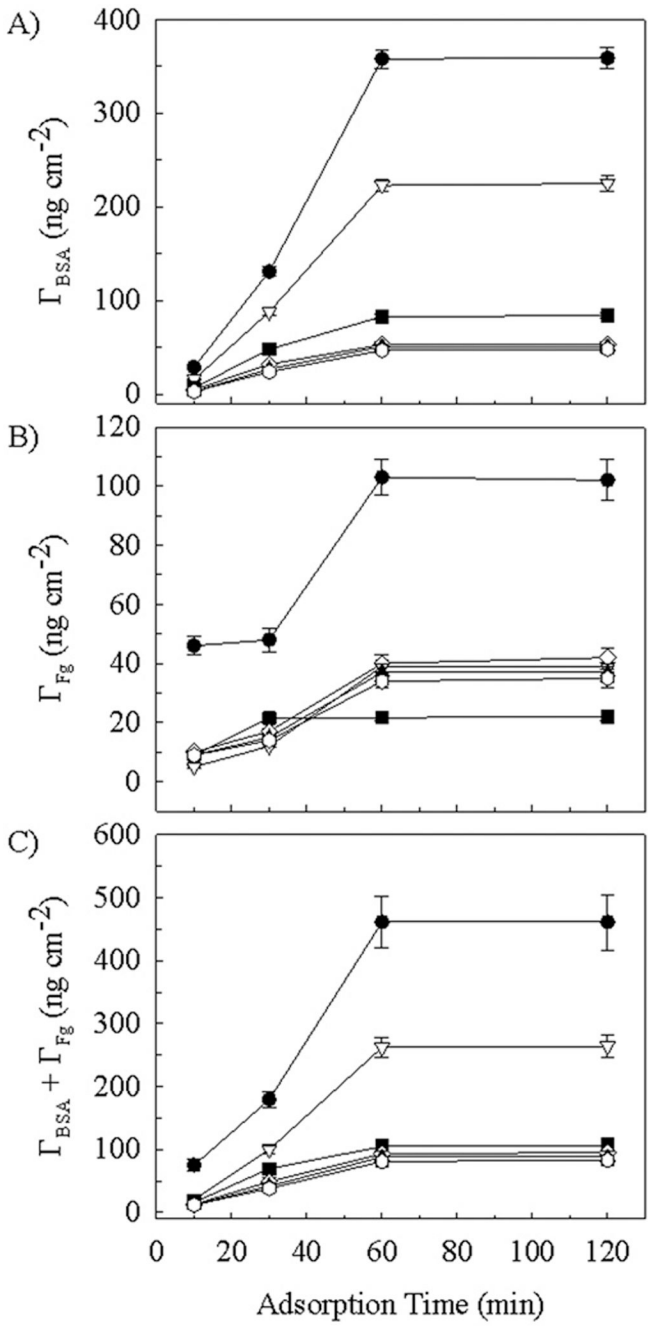

Figure 7.

Protein surface density Γ on (●) bare silicon, (▽) 4 h dextranized silicon, (■) 0.5 h dextranized silicon, (◊) human hyaluronized (1.2 mg ml^{-1}), (▲) rooster hyaluronized (1.2 mg ml^{-1}) and (⬣) zoo hyaluronized (1.2 mg ml^{-1}) silicon surfaces. Adsorption was from 50/50 mixtures of BSA and Fg at 20 μg ml^{-1} each. Panels are: (A) BSA surface concentration; (B) Fg surface concentration and (C) Total protein surface concentration.

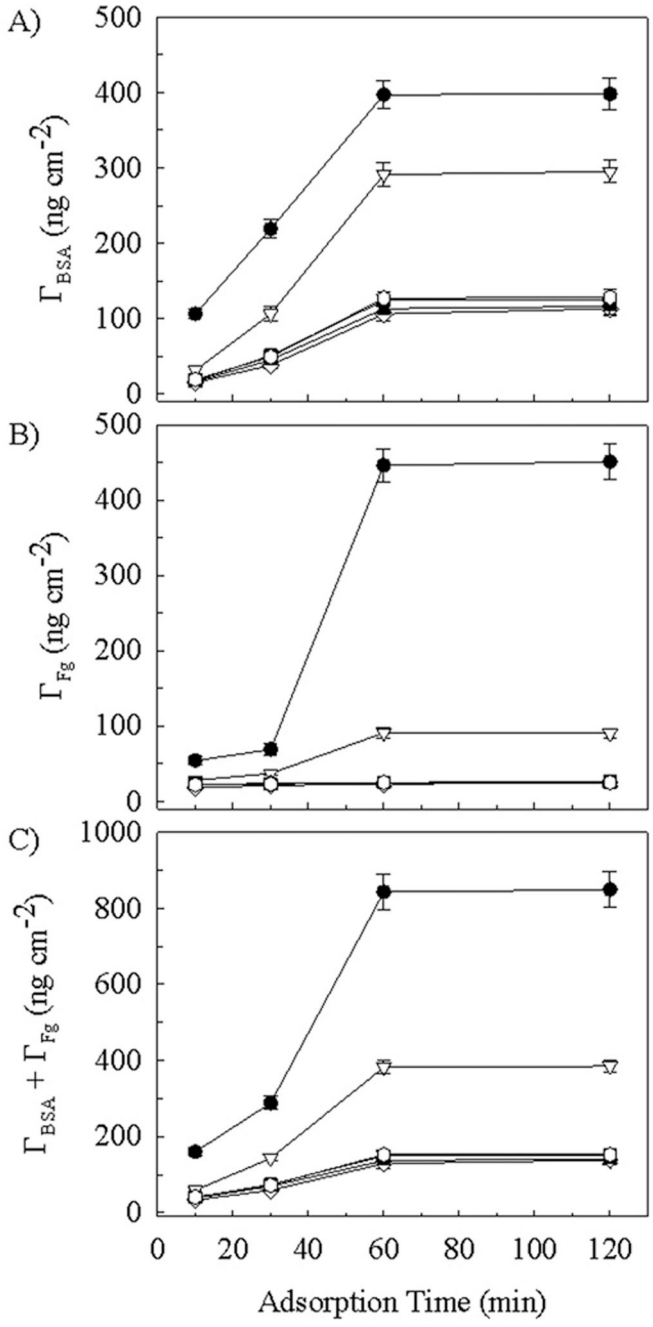

Figure 8.

Protein surface density Γ on (●) bare silicon, (▽) 4 h dextranized silicon, (■) 0.5 h dextranized silicon, (◊) human hyaluronized (1.2 mg ml^{-1}), (▲) rooster hyaluronized (1.2 mg ml^{-1}) and (⬣) zoo hyaluronized (1.2 mg ml^{-1}) silicon surfaces. Adsorption was from 50/50 mixtures of BSA and Fg at 40 μg ml^{-1} each. Panels are: (A) BSA surface concentration; (B) Fg surface concentration and (C) Total protein surface concentration.

Table 1

Water contact angle of bare, dextranized and hyaluronized surfaces subjected to 1 h of adsorption. Protein concentrations were 20 μg ml^{-1}.

	Silicon	Dextran		NaHA		
Solution		**0.5h**	**4h**	**Human**	**Rooster**	**Zoo**
H_20	0	40.4 ± 1.0	53.1 ± 1.4	21.9 ± 1.7	22.4 ± 1.6	22.6 ± 1.7
PBS	0	34.1 ± 3.4	47.2 ± 2.9	23.1 ± 1.6	21.9 ± 1.5	22.5 ± 1.6
PBS+Fg	64.7 ± 2.9	50.2 ± 1.3	56.5 ± 1.7	39.2 ± 1.8	39.6 ± 1.7	38.8 ± 1.8
PBS+BSA	68.9 ± 3.1	52.2 ± 2.2	57.9 ± 1.8	43.0 ± 1.8	41.3 ± 1.9	40.8 ± 1.7
PBS+BSA+Fg	69.5 ± 2.8	56.0 ± 3.0	61.7 ± 3.3	43.5 ± 2.2	41.8 ± 2.4	41.1 ± 2.6